

Optimal Positioning of Flying Relays for Wireless Networks: A LOS Map Approach

Junting Chen and David Gesbert

Communication Systems Department, EURECOM, Sophia Antipolis, France

Email:{chenju, gesbert}@eurecom.fr

Abstract—This paper considers the exploitation of unmanned aerial vehicles (UAVs) in wireless networking, with which communication-enabled robots operate as flying wireless relays to help fill coverage or capacity gaps in the network. We focus on the particular problem of (automatic) UAV positioning, which is known to crucially affect performance. Existing methods typically rely on statistical models of the air-to-ground channel, and thus, they fail to exploit the fine-grained information of line-of-sight (LOS) conditions at some locations. This paper develops an efficient algorithm to find the best position of the UAV based on the fine-grained LOS information. In spite of the complex terrain topology, the algorithm is able to converge to the optimal UAV position to maximize the end-to-end throughput without a global exploration of a signal strength radio map. Numerical results demonstrate that in a dense urban area, the UAV-aided wireless system with the optimal UAV position can almost double the end-to-end capacity from the base station (BS) to the user as compared to that of a direct BS to user link.

I. INTRODUCTION

The throughput demand in wireless cellular networks has dramatically increased in recent years. Along with the rapid development of traditional cellular network infrastructure, there have been tremendous research efforts and commercial applications of UAVs. One promising application is to exploit communication-enabled UAVs as relays in the air to expand the coverage and capacity of the cellular network when and where it matters the most [1], [2].

Clearly, the position of the UAV affects the link strength on both the BS-UAV and UAV-user links. Prior works considered various strategies for optimal UAV positioning. The works [3]–[5] optimized the position of the UAV to balance the links to the BS and to the users assuming LOS propagation. In addition, the works [6]–[8] developed a statistical channel model to capture the insights that the higher the UAV is, the higher probability it might experience in LOS propagation to the user. With that, they optimized the UAV position to balance the coverage and the power consumption.

However, most existing works are based on macroscopic statistical channel models, which do not capture the fine structure of the LOS propagation due to the urban topology. For example, the works [3]–[5] assumed LOS propagations with global averaged path loss models. Such an assumption may hold true when the UAV flies at very high altitude, in which case, the ground user is unlikely blocked by local obstacles. However, this may not be an interesting UAV application in

cellular networks, because the path loss due to high altitude becomes the performance bottleneck. In addition, the works [6]–[9] considered a statistical model, where the probability that the UAV-user link experiences in LOS propagation depends on the height of the UAV and the elevation angle at the user. Such an assumption may hold true only when the obstacles, such as buildings and trees, are uniformly distributed. In addition, they fail to exploit the actual propagation at specific UAV and user locations. To our best knowledge, none of the existing works exploit the *fine-grained structure* of the LOS propagation for UAV positioning. For example, a slight change of the UAV position may result in a significant difference in the channel gain because the UAV may enter from LOS to non-line-of-sight (NLOS) propagation to the user due to building edges.

This paper tries to optimize the UAV position by exploiting the fine structure of the UAV-user propagation, where the UAV relay the message from the BS to the user based on a simple decode-and-forward strategy. The fundamental challenge is that since the ground obstacles surrounding the user may have irregular shapes and random locations, a UAV-user signal strength radio map may have irregular structure of the LOS propagation segment, leading to a global exploration problem. Considering online UAV positioning, where the UAV needs to move to the desired spot to explore the propagation opportunity, global exploration of the entire area would require an unacceptably long time. To the best of our knowledge, none of the existing work attempts to find the global optimal UAV position to the fine-grained propagation structure.

In this paper, efficient search algorithms for the optimal UAV position are developed. We exploit a segmented propagation model to capture the air-to-ground channel and discover a *radiation* property for the UAV-user propagation. Conceptually, when the UAV moves at a fixed height straightly towards the user, the number of obstacles between the UAV and the user keeps decreasing and the channel gain improves. Exploiting such a property, the global optimal UAV position can be found without a global exploration, and only linear complexity is required by the proposed algorithm as compared to the quadratic complexity by a global exploration. Numerical results demonstrate that the optimal UAV position brings in 40% throughput gain for the edge users over a simple UAV position algorithm, and 100% throughput gain over the direct BS-user link.

II. SYSTEM MODEL

Consider a cellular network deployed in a dense urban environment, where the BS locates on the rooftop of a building with height H_B above the ground. Denote the coordinate of the BS as $\mathbf{x}_B = (0, 0, H_B)$. Suppose the BS serves a user with fixed position surrounding by some obstacles, such as buildings or trees. The user can be considered as a wireless device with temporary fixed position or a relay BS without a backhaul. A UAV flies in the sky with a fixed height H_D to relay the signal between the BS and the user. Similarly, denote the coordinates of the UAV and the user as $\mathbf{x}_D = (\bar{\mathbf{x}}_D, H_D)$ and $\mathbf{x}_U = (\bar{\mathbf{x}}_U, H_U)$, respectively, where $\bar{\mathbf{x}}_D, \bar{\mathbf{x}}_U \in \mathbb{R}^2$.

A. The Air-to-ground Channel Model

1) *BS-UAV Channel*: Consider that the heights H_B and H_D are large enough such that there is always LOS propagation between the BS and the UAV. Define the *channel* as the power response averaged over the small scale fading. The BS-UAV channel is modeled as

$$g_B(\mathbf{x}_D) = \beta_0 \|\mathbf{x}_D - \mathbf{x}_B\|^{-\alpha_0} \quad (1)$$

where $\alpha_0 > 1$, $\beta_0 > 0$ are some parameters known by the system.

2) *UAV-user Channel*: We consider a segmented ray-tracing propagation model for the UAV-user channel [10], to distinguish different propagation segments, such as LOS, obstructed LOS [11], and NLOS, according to the UAV and user locations.¹

Specifically, let $\mathbb{D} \subseteq \mathbb{R}^6$ be the domain of all possible UAV-user location pairs $(\mathbf{x}_D, \mathbf{x}_U)$. Consider a partition of \mathbb{D} into K disjoint segments; i.e., $\mathbb{D} = \mathcal{D}_1 \cup \mathcal{D}_2 \cup \dots \cup \mathcal{D}_K$, where $\mathcal{D}_k \cap \mathcal{D}_j = \emptyset$, for $k \neq j$. The UAV-user channel is modeled as

$$g_D(\mathbf{x}_D) = \sum_{k=1}^K \beta_k \|\mathbf{x}_D - \mathbf{x}_U\|^{-\alpha_k} \mathbb{I}\{(\mathbf{x}_D, \mathbf{x}_U) \in \mathcal{D}_k\} \quad (2)$$

where $\alpha_k > 1$, $\beta_k > 0$, and $\mathbb{I}\{A\}$ is an indicator function taking value 1 if condition A is satisfied, and 0 otherwise.

The parameters α_k and β_k describe the model of the average path loss incorporating the shadowing effect for the k th segment. Assume that the functions (1) and (2) are completely known; i.e., the segments $\{\mathcal{D}_k\}$ and the parameters $\{\alpha_k, \beta_k\}$ are known by the system. Note that these parameters can be estimated on the fly during an online implementation.

B. Assumptions and the Polar Coordinate

We make the following mild assumptions in order to focus on the first-order effect of the propagation (e.g., whether it is a LOS propagation).

Let d_0 be the minimum distance between the UAV and the user.

¹Note that with more segments to be classified, the shadowing in each segment has less variance [10], [11], and the segmented model (2) becomes more accurate to the actual channel.

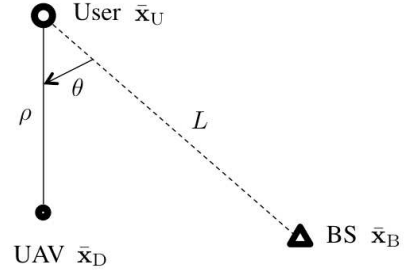


Figure 1. Illustration of a polar representation of $\bar{\mathbf{x}}_D$.

Assumption 1 (Ordered propagation segments): Given $d \geq d_0$, the following holds

$$\beta_k d^{-\alpha_k} > \beta_j d^{-\alpha_j}$$

for $1 \leq k < j \leq K$. ■

For example, under $K = 2$, the propagation can be characterized by $k = 1$ for LOS segment and $k = 2$ for NLOS segment, and the above assumption says that given the same distance d , the LOS scenario yields a higher channel gain compared to the NLOS scenario.

The physical meaning of Assumption 1 can be interpreted as follows: a small k corresponds to the propagation where the signal penetrates light obstacles, such as trees, whereas a large k corresponds to the propagation where the signal penetrates heavy obstacles, such as concrete walls. In addition, $k = 1$ implies the LOS propagation.

Consider a polar representation of the UAV position $\bar{\mathbf{x}}_D$ on the xy -plane as illustrated in Fig. 1. Let

$$\bar{\mathbf{x}}_D(\rho, \theta) = \bar{\mathbf{x}}_U + \rho \begin{bmatrix} \cos \theta & -\sin \theta \\ \sin \theta & \cos \theta \end{bmatrix} \frac{\bar{\mathbf{x}}_B - \bar{\mathbf{x}}_U}{\|\bar{\mathbf{x}}_B - \bar{\mathbf{x}}_U\|} \quad (3)$$

where ρ denotes the projected UAV-user distance on the xy -plane, θ is the angle projected on the xy -plane towards the user using the BS-user direction as the reference, and $\bar{\mathbf{x}}_B = (0, 0)$ is the position of the BS on the xy -plane. Given θ , as ρ decreases, the UAV moves towards the user under a fixed height. As we consider a fixed UAV height H_D , the polar coordinate (ρ, θ) can fully describe the UAV position \mathbf{x}_D .

With the polar representation, we make the following mild assumption on the propagation.

Assumption 2 (No significant reflection): Let $\mathbf{x}_D = (\bar{\mathbf{x}}_D(\rho, \theta), H_D)$ and $\mathbf{x}_D' = (\bar{\mathbf{x}}_D(\rho', \theta), H_D)$. Suppose $(\mathbf{x}_D, \mathbf{x}_U) \in \mathcal{D}_k$. Then for $\rho' > \rho$, it holds that $(\mathbf{x}_D', \mathbf{x}_U) \in \mathcal{D}_j$, where $j \geq k$. By contrast, for $0 \leq \rho' < \rho$, it holds that $(\mathbf{x}_D', \mathbf{x}_U) \in \mathcal{D}_j$, where $j \leq k$. ■

For example, under two propagation segments, when the UAV moves away from the user with a fixed θ , it may probably enters from LOS propagation to NLOS propagation. As it moves further away, it only stays in the NLOS segment. A geometric illustration is given in Fig. 2. When the UAV passes the critical point $\rho_{1,2}^B(\theta)$ and moves towards the left, the UAV-user signal will be blocked by more and more obstacles. When the UAV moves towards the right from $\rho_{1,2}^B(\theta)$, it always has LOS propagation to the user.

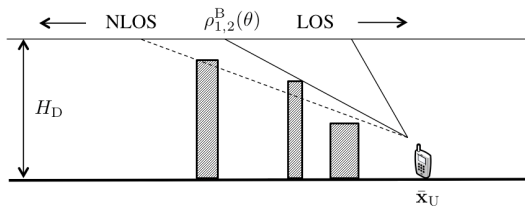


Figure 2. Illustration on the absence-of-significant-reflection assumption, where the UAV moves under a fixed θ .

Assumption 2 can be justified by the *nonexistence-of-significant-reflection* argument. From the geometry as in Fig. 2, as ρ increases, the number of obstacles between the UAV and the user also increases. This contributes to larger path loss exponent α or smaller gain coefficient β , if there is no strong enough reflective or diffractive signals to compensate for the additional loss due to penetrating through additional obstacles. By contrast, when ρ decreases, the number of obstacles between the UAV and the user decreases. Note that such observation is roughly consistent to the channel measurement results reported in [11].

C. Problem Formulation for Optimal UAV Position

The objective of the UAV positioning is to establish a good relay channel from the BS to the user via the UAV. Specifically, a power minimization for UAV positioning is formulated as follows:

$$(P1) \quad \underset{\mathbf{x}_D, p_B, p_D}{\text{minimize}} \quad \omega p_B + (1 - \omega) p_D \quad (4)$$

$$\text{subject to} \quad \log_2 \left(1 + p_B \cdot g_B(\mathbf{x}_D) \right) \geq R_B \quad (5)$$

$$\log_2 \left(1 + p_D \cdot g_D(\mathbf{x}_D) \right) \geq R_D \quad (6)$$

$$p_B, p_D \geq 0$$

where $0 < \omega < 1$ is the parameter to weight the power consumption p_B at the BS and the power consumption p_D at the UAV, the parameters R_B and R_D are the rate requirements for the BS-UAV link and the UAV-user link, respectively.

In addition, an end-to-end rate maximization for UAV positioning is formulated as follows:

$$(P2) \quad \underset{\mathbf{x}_D}{\text{maximize}} \quad \min \{ r_B(\mathbf{x}_D), r_D(\mathbf{x}_D) \} \quad (7)$$

where

$$r_B(\mathbf{x}_D) = \log_2 \left(1 + P_B \cdot g_B(\mathbf{x}_D) \right)$$

$$r_D(\mathbf{x}_D) = \log_2 \left(1 + P_D \cdot g_D(\mathbf{x}_D) \right)$$

in which, the parameters P_B and P_D are the transmission powers at the BS and the UAV, respectively.

Moreover, this paper focuses on the outdoor scenario for the users.

Assumption 3 (Outdoor scenario): There is a LOS propagation from the UAV to the user when the UAV locates on top of the user, i.e., $\bar{\mathbf{x}}_D = \bar{\mathbf{x}}_U$. ■

The above assumption is to avoid discussing the complicated scenario where there may be a good propagation link to the user inside a building through a window.

It is worthy to point out that even with the above assumptions, it is still highly non-trivial to find the optimal UAV position. A numerical example is given in Fig. 3, where a user surrounded by a number of buildings is depicted in Fig. 3 (a). Fig. 3 (b) simulates the received power of users 1 at the UAV corresponding to every UAV position. The irregular pattern is due to the shapes of the buildings. Fig. 3 (c) shows the corresponding capacity from the BS to the user via the UAV. By considering the actual blockage of the buildings, it is not straight forward to identify the best position of the UAV.

III. OPTIMAL UAV POSITION VIA SMART EXPLORATION

We first derive algorithms for the power minimization problem (P1). We then show that the same algorithm can solve the rate maximization problem (P2) under problem reformulations.

A. Problem Reformulation for (P1)

Observed from (P1) that under optimal power allocation p_B and p_D , the two rate constraints (5) and (6) must be active; i.e., the equalities hold. This is because if the channel capacities on the left hand side of (5) and (6) are greater than the rate requirements on the right hand side, then either p_B or p_D can be reduced to yield a lower objective value. With this insight, solving the equations from (5) and (6), the minimum power to satisfy the rate constraint is given by

$$p_B(\mathbf{x}_D) = (2^{R_B} - 1) g_B(\mathbf{x}_D)^{-1}$$

and

$$p_D(\mathbf{x}_D) = (2^{R_D} - 1) g_D(\mathbf{x}_D)^{-1}.$$

In addition, let $d_B \triangleq \|\mathbf{x}_D - \mathbf{x}_B\|$ and $d_U \triangleq \|\mathbf{x}_D - \mathbf{x}_U\|$. Applying the polar representation in (3), we obtain

$$d_B(\rho, \theta) = \sqrt{\rho^2 + L^2 - 2\rho L \cos \theta + (H_D - H_B)^2} \quad (8)$$

$$d_U(\rho) = \sqrt{\rho^2 + (H_D - H_U)^2} \quad (9)$$

where $L \triangleq \|\bar{\mathbf{x}}_U\|$ is the projected distance between the user and the BS on the xy -plane.

Exploiting the channel models (1) and (2), problem (P1) can be reformulated as follows,

$$\underset{\rho \geq 0, \theta}{\text{minimize}} \quad \omega_B \beta_0^{-1} d_B(\rho, \theta)^{\alpha_0} + \omega_D \sum_{k=1}^K \beta_k^{-1} d_U(\rho)^{\alpha_k} \mathbb{I}\{(\rho, \theta) \in \mathcal{P}_k\}$$

where $\omega_B = \omega(2^{R_B} - 1)$, $\omega_D = (1 - \omega)(2^{R_D} - 1)$, and

$$\mathcal{P}_k \triangleq \{(\rho, \theta) : (\mathbf{x}_D(\rho, \theta), \mathbf{x}_U) \in \mathcal{D}_k\}.$$

When the UAV-user pair $(\mathbf{x}_D(\rho, \theta), \mathbf{x}_U)$ is in the k th propagation segment, the objective function is given by

$$F_k(\rho, \theta) \triangleq \omega_B \beta_0^{-1} d_B(\rho, \theta)^{\alpha_0} + \omega_D \beta_k^{-1} d_U(\rho)^{\alpha_k}. \quad (10)$$

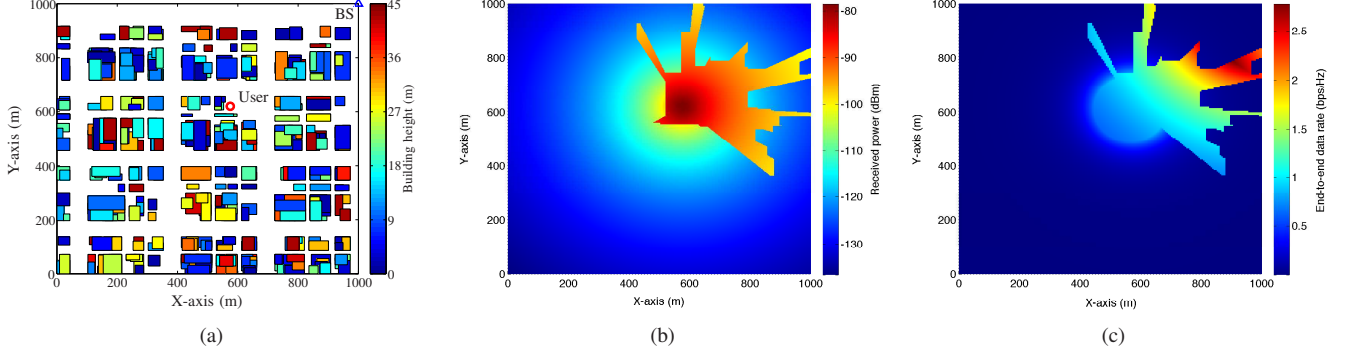


Figure 3. (a) A map of a dense urban area, where the rectangles denote the building with colors representing their heights. (b) The received power map corresponding to every UAV position. (c) The end-to-end capacity map.

The power minimization problem can be further simplified as follows:

$$(P1') \quad \underset{\rho \geq 0, \theta}{\text{minimize}} \quad F(\rho, \theta)$$

where

$$F(\rho, \theta) = \sum_{k=1}^K F_k(\rho, \theta) \mathbb{I}\{(\rho, \theta) \in \mathcal{P}_k\}.$$

B. Properties

We study several important properties of problem (P1').

Proposition 1 (Convexity): Given θ , the functions $F_k(\rho, \theta)$ are convex in ρ .

Denote $\rho_k^*(\theta)$ as the optimal solution to the following problem

$$\underset{\rho \geq 0}{\text{minimize}} \quad F_k(\rho, \theta).$$

Due to the convexity of $F_k(\rho, \theta)$ in ρ , the function $\rho_k^*(\theta)$ can be computed efficiently. For example, a bisection search algorithm can be applied to compute $\rho_k^*(\theta)$ for a given θ .

Proposition 2: Given ρ and θ , the following holds

$$F_k(\rho, \theta) < F_j(\rho, \theta)$$

for $1 \leq k < j \leq K$.

The result in Proposition 2 is straight forward, and it confirms that in terms of power minimization, the propagation segment with smaller k is more favorable.

Proposition 3 (Search region): The optimal solution to (P1') is in the region

$$\mathcal{P} = \left\{ (\rho, \theta) : 0 \leq \rho \leq L \cos \theta, -\frac{\pi}{2} \leq \theta \leq \frac{\pi}{2} \right\}.$$

The above property establishes a stopping criterion for the search algorithm. In addition, we derive another stopping criterion as follows.

Proposition 4 (Local optimality): For $\hat{\theta} \geq 0$, the following property holds

$$\min_{\rho \geq 0} F_k(\rho, \hat{\theta}) \leq \min_{j \geq k} \min_{\rho \geq 0, \hat{\theta} < \theta \leq \frac{\pi}{2}} F_j(\rho, \theta) \quad (11)$$

for $1 \leq k \leq K$. Similarly, for $\hat{\theta} < 0$,

$$\min_{\rho \geq 0} F_k(\rho, \hat{\theta}) \leq \min_{j \geq k} \min_{\rho \geq 0, -\frac{\pi}{2} \leq \theta < \hat{\theta}} F_j(\rho, \theta) \quad (12)$$

Proposition 4 implies the following. If a UAV locates itself at $(\rho_k^*(\hat{\theta}), \hat{\theta})$ that is found to minimize $F_k(\rho, \hat{\theta})$, and it is at the k th propagation segment, i.e., $(\rho_k^*(\hat{\theta}), \hat{\theta}) \in \mathcal{P}_k$, then it is not possible to further lower the objective $F(\rho, \theta)$ in the region $\theta > \hat{\theta}$, for $\hat{\theta} > 0$ (or $\theta < \hat{\theta}$, for $\hat{\theta} < 0$), unless it finds a propagation segment $j < k$ in $\theta > \hat{\theta}$, for $\hat{\theta} > 0$ (or $\theta < \hat{\theta}$, for $\hat{\theta} < 0$). In particular, for $k = 1$, there is no need to search in the region $\theta > \hat{\theta}$, for $\hat{\theta} > 0$ (or $\theta < \hat{\theta}$, for $\hat{\theta} < 0$).

Let $\rho_{k,j}^B(\theta)$, $k < j$, denote the boundary point that separates the k th and j th propagation segments; i.e., for $\rho = \rho_{k,j}^B(\theta) - \epsilon$, we have $(\rho, \theta) \in \mathcal{P}_k$, and for $\rho = \rho_{k,j}^B(\theta) + \epsilon$, $(\rho, \theta) \in \mathcal{P}_j$, where $\epsilon > 0$ is a sufficiently small positive number. Following Assumptions 2 and 3, it is found that the propagation segments follow radiated patterns centered at the user. In addition, the radiated propagation segments do not overlap but contain one and the other.

Proposition 5 (Radiated propagation pattern): For $0 \leq \rho < \rho_{k,j}^B(\theta)$, we have $(\rho, \theta) \in \mathcal{P}_m$, $m \leq k$, and for $\rho > \rho_{k,j}^B(\theta)$, we have $(\rho, \theta) \in \mathcal{P}_n$, $n \geq j$.

A numerical example of the radiated propagation pattern is illustrated in Fig. 3 (b).

For mathematical convenience, we define the boundary point $(\rho_{k,j}^B(\theta), \theta) \in \mathcal{P}_k$.

C. Algorithm for $K = 2$ Case

In this paper, we study the case of two propagation segments, and the general case is left for future works. The algorithm for optimal UAV positioning is derived using the intuitions from Propositions 1–5.

For easy elaboration, we call the first segment as the LOS segment and the second segment as the NLOS segment. The basic idea is to discover the LOS segment and find a good position in it. Towards this end, the algorithm searches along the contour $F_1(\rho, \theta) = C$ when (ρ, θ) is in the NLOS segment \mathcal{P}_2 . When (ρ, θ) is in the LOS segment \mathcal{P}_1 , the algorithm moves under a fixed θ . Specifically, the procedure is described in Algorithm 1.

Algorithm 1 Optimal UAV positioning for minimum power consumption for $K = 2$

- Initialization: Let $\theta = 0$. Choose $\rho \in \{\rho_1^*(0), \rho_2^*(0), \rho_{1,2}^B(0)\}$ that yields the minimum objective value $F(\rho, 0)$. Choose a step size $\delta > 0$. Repeat the following two search phases until one of the stopping criteria is met.
- Phase I (Search in the NLOS segment): When $(\rho, \theta) \in \mathcal{P}_2$, search along the contour $F_1(\rho, \theta) = C$; i.e., update the position $\rho \leftarrow \rho + d\rho$, $\theta \leftarrow \theta + d\theta$, where $d\rho$ and $d\theta$ are unique solutions to the following equations

$$\frac{\partial F_1(\rho, \theta)}{\partial \rho} d\rho + \frac{\partial F_1(\rho, \theta)}{\partial \theta} d\theta = 0 \quad (13)$$

$$\rho^2 + (\rho + d\rho)^2 - 2\rho(\rho + d\rho) \cos(d\theta) = \delta^2 \quad (14)$$

$$d\theta > 0 \quad (15)$$
- Phase II (Search in the LOS segment): When $(\rho, \theta) \in \mathcal{P}_1$, change ρ towards $\rho_{1,2}^B(\theta)$ by δ ; i.e., $\rho \leftarrow \rho + \delta$ if $\rho < \rho_{1,2}^B(\theta)$, and $\rho \leftarrow \rho - \delta$, otherwise.
- Stopping criteria: (i) $\rho \geq L \cos \theta$, and (ii) $|\rho - \rho_1^*(\theta)| \leq \delta$.
- Optimal position: For each step, the algorithm keeps a record of the minimum objective value F_{\min} ; i.e., $F_{\min} \leftarrow F(\rho, \theta)$, $(\hat{\rho}, \hat{\theta}) \leftarrow (\rho, \theta)$, if $F(\rho, \theta) < F_{\min}$.

It turns out that the above algorithm terminates after finite steps, and it converges to the neighborhood of the optimal UAV position as summarized in the following theorem.

Theorem 1 (Convergence): For every $\epsilon > 0$, there exists a $\bar{\delta} > 0$, such that for $\delta < \bar{\delta}$, the iterate $(\hat{\rho}, \hat{\theta})$ in Algorithm 1 converges to an ϵ -neighborhood of the optimal point (ρ^*, θ^*) as the solution to

$$\underset{\rho \geq 0, 0 \leq \theta \leq \frac{\pi}{2}}{\text{minimize}} \quad F(\rho, \theta)$$

in $\mathcal{O}(L\delta^{-1})$ steps.

Similarly, if we change the search direction constraint (15) in Algorithm 1 to $d\theta < 0$, we can obtain the optimal solution (ρ^*, θ^*) as minimizing $F(\rho, \theta)$ over $\rho \geq 0$ and $-\frac{\pi}{2} \leq \theta \leq 0$. To compare the minimum objective value $F_{\min}^{(1)}$ and $F_{\min}^{(2)}$ obtained under $d\theta > 0$ and $d\theta < 0$ from Algorithm 1, respectively, we can obtain the global optimal solution to problem (P1').

Theorem 1 demonstrates the efficiency of the algorithm, which is linear in the geographical scale L . Note that without a smart design, an exhaustive search algorithm may need $\mathcal{O}(L^2\delta^{-1})$ steps. Therefore, the proposed algorithm has significantly reduce the complexity for the online search for the optimal UAV position.

D. UAV Position Algorithm for (P2)

Let $r_B(\rho, \theta) = \log_2(1 + P_B \cdot \beta_0 d_B(\rho, \theta)^{-\alpha_0})$ and $r_{D,k}(\rho) = \log_2(1 + P_D \cdot \beta_k d_U(\rho)^{-\alpha_k})$. In addition, let

$$F_k(\rho, \theta) = -\min\{r_B(\rho, \theta), r_{D,k}(\rho)\} \quad (16)$$

and

$$F(\rho, \theta) = \sum_{k=1}^K F_k(\rho, \theta) \mathbb{I}\{(\rho, \theta) \in \mathcal{P}_k\}.$$

Then problem (P2) can be equivalently transformed into problem (P1').

For the capacity optimization (P2), although the function $F_k(\rho, \theta)$ defined in (16) is not concave, the optimal solution $\rho_k^*(\theta)$ that maximizes $F_k(\rho, \theta)$ over $0 \leq \rho \leq L \cos \theta$ can still be found using bisection search. This is because for a fixed θ , $r_B(\rho, \theta)$ is an increasing function over $0 \leq \rho \leq L \cos \theta$, and $r_{D,k}(\rho)$ is a decreasing function over $\rho \geq 0$. Moreover, the optimality condition for $\rho_k^*(\theta)$ is $r_B(\rho_k^*, \theta) = r_{D,k}(\rho_k^*)$.

One can easily verify that Propositions 2–4 still hold. In addition, Proposition 5 is independent to the objective functions. With these insights, Algorithm 1 can be applied to find the optimal UAV position for the capacity maximization problem (P2). In addition, we can show that the same convergence result in Theorem 1.

IV. NUMERICAL RESULTS

Consider a dense urban area with buildings ranging from 5–45 meter height as illustrated in Fig. 3 (a). The user is represented by a red circle and the BS locates at the top right corner denoted by a blue triangle. The height of the BS is 45 meters, and the UAV moves at 50 meter height. As a result, there is always LOS propagation between the UAV and the BS. Consider two propagation scenarios depending on whether there is LOS propagation between the UAV and the user. Correspondingly, the parameters for the channel models (1) and (2) are chosen as $(\alpha_0, \beta_0, \alpha_1, \beta_1, \alpha_2, \beta_2) = (2.2, 10^{-4}, 2.3, 10^{-4}, 3.6, 10^{-3})$ according to some proper scenarios chosen from the WINNER II channel model.

We evaluate the UAV positioning algorithm for the end-to-end capacity maximization problem (P2). The transmission powers are chosen as $P_B = 30$ dBm and $P_D = 36$ dBm, and the noise power is -70 dBm. The corresponding power map and end-to-end capacity map for every UAV position are illustrated in Fig. 3 (b) and (c).

In Fig. 4 the green curves show the search path for the optimal UAV position, where the two branches correspond to the searches over $d\theta > 0$ and $d\theta < 0$ in Algorithm 1, respectively. The other curves represent the contour for equal end-to-end capacity, where the red contour represents the highest capacity. The optimal UAV position is found at the purple diamond.

Consider that a user locates randomly and uniformly on the streets depicted in Fig. 3 (a). A UAV is placed at the optimal position from Algorithm 1 to relay the BS and the user. The proposed scheme is compared to the following baselines:

- **Direct BS-user transmission:** The BS directly transmits to the user without relaying via the UAV.
- **Offline UAV positioning:** First, obtain the empirical distribution of the LOS propagation $\mathbb{P}\{\text{LOS}|\varphi\}$ given the elevation angle φ at the user placed at a uniformly random location on the streets in Fig. 3 (a). Then, for each UAV

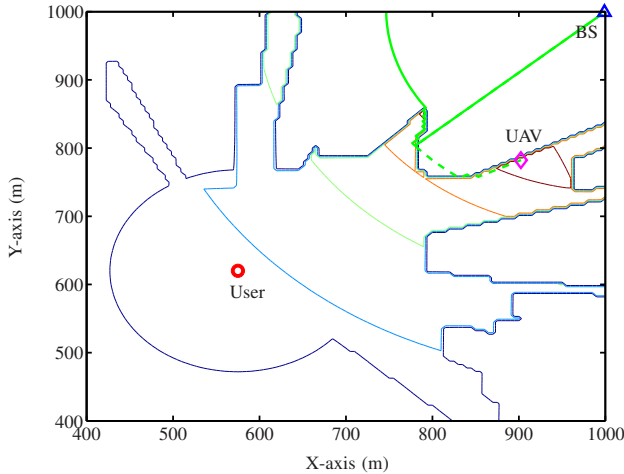


Figure 4. Search path (greed lines) towards the optimal UAV position (purple diamond). The curves in other colors represent the contour of the end-to-end capacity (7) in (P2).

position \mathbf{x}_U , calculate the elevation angle $\varphi(\mathbf{x}_D, \mathbf{x}_U)$, and compute the average UAV-user channel as [8], [9]

$$g_D(\mathbf{x}_D) = \mathbb{P}\{\text{LOS}|\varphi\}\beta_1\|\mathbf{x}_D - \mathbf{x}_U\|^{-\alpha_1} + \left(1 - \mathbb{P}\{\text{LOS}|\varphi\}\right)\beta_2\|\mathbf{x}_D - \mathbf{x}_U\|^{-\alpha_2}.$$

Based on the above average channel, obtain the optimal UAV position by maximizing the end-to-end capacity (7).

- **Simple UAV positioning:** Obtain the optimal UAV position by searching along with the line segment between the BS and the user (i.e., implement only the initialization step in Algorithm 1).

Fig. 5 compares the average end-to-end throughput over 10,000 user drops on the streets in Fig. 3 (a). The cell edge users are recognized as those within the 20th percentile of the throughput under direct BS-user transmission. First, across all the three user categories, the proposed scheme with the optimal UAV placement achieves the highest throughput. In particular for the cell edge users, the proposed scheme doubles the throughput. Second, the proposed scheme achieves over 40% throughput gain at cell edge users over the simple UAV positioning scheme without significantly extending the search trajectory. Third, the offline UAV positioning scheme does not perform well since it only exploits statistical information.

V. CONCLUSION

This paper studied optimal UAV positioning problems for a UAV-relayed wireless communication system in a dense urban area. The UAV searches and exploits the opportunity of a LOS propagation towards the user, while maintaining a good connection with the BS, such that transmission power is minimized or the end-to-end capacity is maximized. By studying several properties of the problems, an efficient algorithm was derived to search for the global optimal UAV position in a few number of steps that scales linearly to the geographical scale

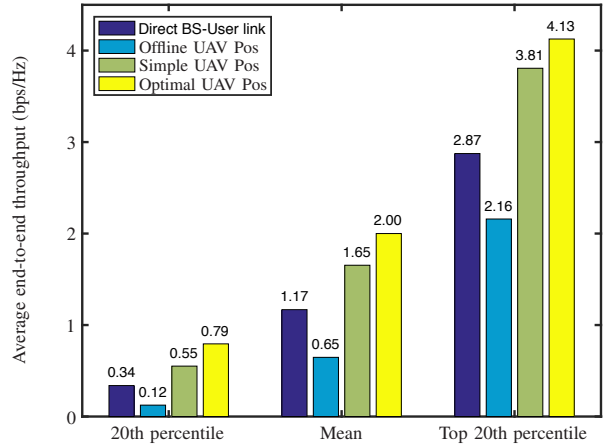


Figure 5. Comparison of the average end-to-end throughput over different schemes.

of the search area. Numerical results demonstrated significant throughput gain over simple UAV position algorithms.

ACKNOWLEDGMENT

This work was supported by the ERC under the European Union's Horizon 2020 research and innovation program (Agreement no. 670896).

REFERENCES

- [1] Y. Zeng, R. Zhang, and T. J. Lim, "Wireless communications with unmanned aerial vehicles: opportunities and challenges," *IEEE Commun. Mag.*, vol. 54, no. 5, pp. 36–42, 2016.
- [2] D.-T. Ho, P. Sujit, T. A. Johansen, and J. B. De Sousa, "Performance evaluation of cooperative relay and particle swarm optimization path planning for UAV and wireless sensor network," in *Proc. IEEE Globecom Workshops*, 2013, pp. 1403–1408.
- [3] O. Jian, Z. Yi, L. Min, and L. Jia, "Optimization of beamforming and path planning for UAV-assisted wireless relay networks," *Chinese Journal of Aeronautics*, vol. 27, no. 2, pp. 313–320, 2014.
- [4] Y. Jin, Y. D. Zhang, and B. K. Chalise, "Joint optimization of relay position and power allocation in cooperative broadcast wireless networks," in *Proc. IEEE Int. Conf. Acoustics, Speech, and Signal Processing*, 2012, pp. 2493–2496.
- [5] D. H. Choi, B. H. Jung, and D. K. Sung, "Low-complexity maneuvering control of a UAV-based relay without location information of mobile ground nodes," in *Proc. IEEE Symposium on Computers and Commun.*, 2014, pp. 1–6.
- [6] M. Mozaffari, W. Saad, M. Bennis, and M. Debbah, "Drone small cells in the clouds: Design, deployment and performance analysis," in *Proc. IEEE Global Telecomm. Conf.*, 2015, pp. 1–6.
- [7] A. Hourani, K. Sithampanathan, and S. Lardner, "Optimal LAP altitude for maximum coverage," *IEEE Commun. Lett.*, no. 99, pp. 1–4, 2014.
- [8] M. Mozaffari, W. Saad, M. Bennis, and M. Debbah, "Optimal transport theory for power-efficient deployment of unmanned aerial vehicles," *arXiv preprint arXiv:1602.01532*, 2016.
- [9] A. Al-Hourani, S. Kandeepan, and A. Jamalipour, "Modeling air-to-ground path loss for low altitude platforms in urban environments," 2014, pp. 2898–2904.
- [10] J. Chen, U. Yatnalli, and D. Gesbert, "Learning radio maps for UAV-aided wireless networks: A segmented regression approach," in *Proc. IEEE Int. Conf. Commun.*, Paris, France, May 2017, to appear.
- [11] Q. Feng, J. McGeehan, E. K. Tameh, and A. R. Nix, "Path loss models for air-to-ground radio channels in urban environments," in *Proc. IEEE Semianual Veh. Technol. Conf.*, vol. 6, 2006, pp. 2901–2905.